

# Panoptic SegFormer

Zhiqi Li<sup>1</sup>, Wenhai Wang<sup>1</sup>, Enze Xie<sup>2</sup>, Zhiding Yu<sup>3</sup>,  
Anima Anandkumar<sup>3,4</sup>, Jose M. Alvarez<sup>3</sup>, Tong Lu<sup>1</sup>, Ping Luo<sup>2</sup>

<sup>1</sup>Nanjing University <sup>2</sup>The University of Hong Kong <sup>3</sup>NVIDIA <sup>4</sup>Caltech

## Abstract

We present *Panoptic SegFormer*, a general framework for end-to-end panoptic segmentation with Transformers. The proposed method extends Deformable DETR with a unified mask prediction workflow for both things and stuff, making the panoptic segmentation pipeline concise and effective. With a ResNet-50 backbone, our method achieves 50.0% PQ on the COCO test-dev split, surpassing previous state-of-the-art methods by significant margins without bells and whistles. Using a more powerful PVTv2-B5 backbone, *Panoptic SegFormer* achieves a new record of 54.1% PQ and 54.4% PQ on the COCO val and test-dev splits with single scale input.

## 1. Introduction

Semantic segmentation and instance segmentation are two important and correlated vision problems. Their underlying connections recently motivated panoptic segmentation as a unification of both tasks [1]. In panoptic segmentation, image contents are divided into two types: things and stuff. Things are countable instances (e.g., person, car, and bicycle) and each instance has a unique id to distinguish it from the other instances. Stuff refers to the amorphous and uncountable regions (e.g., sky, grassland, and snow) and has no instance id [1].

The differences between things and stuff also lead to different ways to handle their predictions. A number of works simply decompose panoptic segmentation into an instance segmentation task for things and a semantic segmentation task for stuff [1–5]. However, such a separated strategy tend to increase model complexity and undesired artifacts. Several works further consider bottom-up (proposal-free) instance segmentation approaches but still maintain similar separate strategies [6–10]. Some recent methods try to simplify the panoptic segmentation pipeline by processing things and stuff with a unified framework. For example, several works [11–14] achieve this with fully convolutional frameworks. These framework share a similar “top-down

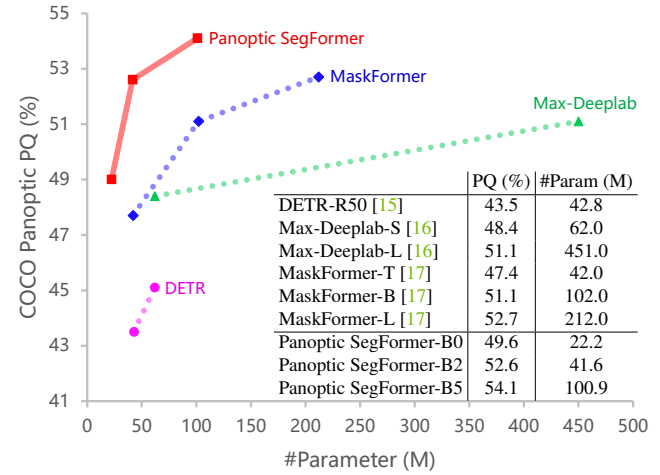


Figure 1: **Comparison to the prior arts in panoptic segmentation methods on the COCO val2017 split.** Under comparable number of parameters, Panoptic SegFormer models outperform the other counterparts among different models. Panoptic SegFormer (PVTv2-B5) achieves a new state-of-the-art 54.1%PQ, outperforming the previous best method MaskFormer by 1.4% with significantly fewer parameters.

meets bottom-up” two-branch design where a kernel branch encodes object/region information, and is dynamically involved with an image-level feature branch to generate the object/region masks.

Recently, Vision Transformers have been widely introduced to instance localization and recognition tasks [15, 18–20]. Vision Transformers generally divide an input image into crops and encode them as tokens. For object detection problems, both DETR [15] and Deformable DETR [18] represent the object proposals with a set of learnable queries which are used to predict bounding boxes and are dynamically matched with object ground truths via a bipartite graph matching loss. The role of query features is similar to RoI features in conventional detection architectures, thus inspiring several methods [15–17] with two-branch designs similar to Panoptic FCN [13].

In this work, we propose Panoptic SegFormer, a concise and effective framework for end-to-end panoptic segmentation with Vision Transformers. Specifically, Panoptic SegFormer contains three key designs:

- A query set to represent things and stuff uniformly, where the stuff classes are considered as special type of things with single instance ids;
- A location decoder which focuses on leveraging the location information of things and stuff to improve the segmentation quality;
- A mask-wise post-processing strategy to equally merge the segmentation results of things and stuff.

Benefiting from these three designs, Panoptic SegFormer achieves state-of-the-art panoptic segmentation performance tasks with efficiency.

To verify our framework, we conduct extensive experiments on the COCO dataset [21]. As shown in Figure 1, our smallest model, Panoptic SegFormer (PVTv2-B0), achieves 49.0% PQ on the COCO val2017 split with only 22.2M parameters, surpassing prior arts such as MaskFormer [17] and Max-Deeplab [16], whose parameter sizes are twice and three times larger. Panoptic SegFormer (PVTv2-B5) further achieves the state PQ of 54.1%, which is 3% PQ higher than Max-Deeplab (51.1% PQ) and 1.4% PQ higher than MaskFormer (52.7% PQ), respectively, while our method still enjoys significantly fewer parameters. It is worth mentioning that Panoptic SegFormer achieves 54.4% PQ on COCO test-dev with single scale input, outperforming competition methods including Innovation [22], which uses plenty of tricks such as model ensemble, multi-scale testing. Currently, Panoptic SegFormer (PVTv2-B5) is the 1st place on COCO Panoptic Segmentation leaderboard<sup>1</sup>.

## 2. Related Work

**Panoptic Segmentation.** The panoptic segmentation literature mainly treat this problem as a joint task of instance segmentation and semantic segmentation where things and stuff are handled separately. Kirillov *et al.* [1] proposed the concept of and benchmark of panoptic segmentation together with a baseline which directly combines the outputs of individual instance segmentation and semantic segmentation models. Since then, models such as Panoptic FPN [2], UPSNet [4] and AUNet [23] have improved the accuracy and reduced the computational overhead by combining instance segmentation and semantic segmentation into a single model. However, these methods still approximate the target task by solving the surrogate sub-tasks, therefore introducing undesired model complexities and sub-optimal performance.

Recently, efforts have been made to unified framework of panoptic segmentation. Li *et al.* [13] proposed Panoptic FCN where the panoptic segmentation pipeline is simplified with a “top-down meets bottom-up” two-branch design similar to CondInst [11]. In their work, things and stuff are jointly modeled by an object/region-level kernel branch and an image-level feature branch. Several recent works represent things and stuff as queries and perform end-to-end panoptic segmentation via transformers. DETR [15] predicts the bounding boxes of things and stuff and combines the attention maps of the transformer decoder and the feature maps of ResNet [24] to perform panoptic segmentation. Max-Deeplab [16] directly predicts object categories and masks through a dual-path transformer regardless of the category being things or stuff. On top of DETR, MaskFormer [17] uses an additional pixel decoder to refine high spatial resolution features and generated the masks by multiplying queries and features from the pixel decoder. Due to the computational complexity of multi-head attention [25], both DETR and MaskFormer use feature maps with limited spatial resolutions for panoptic segmentation, which hurts the performance and requires combining additional high-resolution feature maps in final mask prediction. These methods have provided unified frameworks for predicting things and stuff in panoptic segmentation. However, there is still a noticeable gap between these methods and the top leaderboard methods with separated prediction strategies in terms of performance [22, 26].

**End-to-end Object Detection.** The recent popularity of end-to-end object detection frameworks have inspired many other related works. DETR [15] is arguably the most representative end-to-end object detector among these methods. DETR models the object detection task as a dictionary lookup problem with learnable queries and employs an encoder-decoder transformer to predict bounding boxes without extra post-processing. DETR greatly simplifies the conventional detection framework and removes many hand-crafted components such as NMS [27, 28] and anchors [28]. Zhu *et al.* [18] proposed Deformable DETR which further reduces the memory and computational cost in DETR through deformable attention layers. Although having these advantages, the attention maps of the deformable attention layers are sparse and cannot be directly used for dense prediction in panoptic segmentation.

**Instance Segmentation.** Mask R-CNN [29] has been one of the most representative two-stage instance segmentation methods by first extracting ROIs and then predicting the final results conditioned on these ROIs. One-stage methods such as CondInst [11] and SOLOv2 [12] further simplifies this pipeline by employing dynamic filters (conditional convolution) [30] with a kernel branch. Recently, SOLQ [31]

<sup>1</sup><https://competitions.codalab.org/competitions/19507#results>

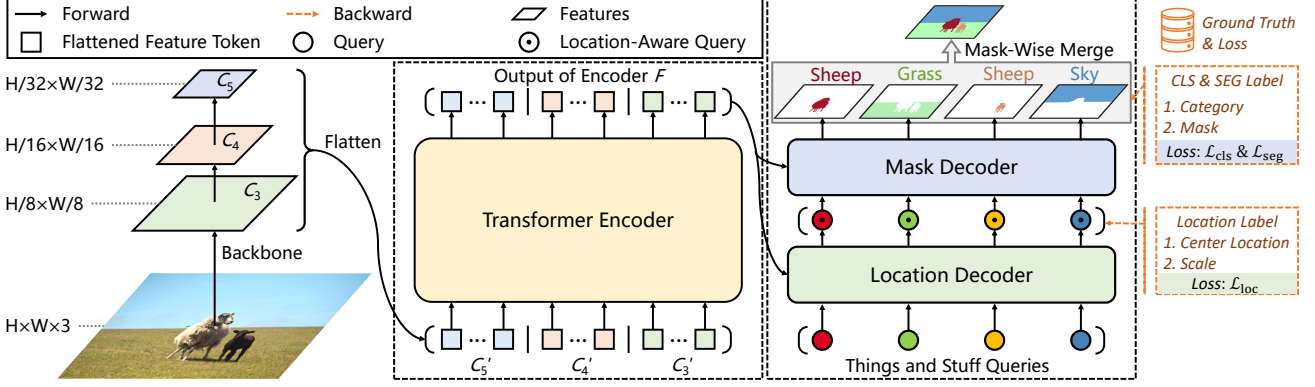


Figure 2: **Overview of Panoptic SegFormer.** Panoptic SegFormer is composed of backbone, encoder, and decoder. The backbone and the encoder output and refines multi-scale features. Inputs of the decoder are  $N$  queries and the multi-scale features. The decoder consists of two sub-decoders: location decoder and mask decoder, where location decoder aims to learn reference points of queries, and mask decoder predicts the final category and mask. Details of the decoder will be introduced below. We use a mask-wise merging method instead of the commonly used pixel-wise argmax method to perform inference.

and QueryInst [32], perform instance segmentation in an end-to-end paradigm without involving NMS. QueryInst is based on an end-to-end object detector Sparse-RCNN [33] and predicts masks through corresponding bounding boxes and queries. By encoding masks to vectors, SOLQ predicts mask vectors in a regressive manner and outputs the final masks by decoding the vectors. The proposed Panoptic SegFormer can also handle end-to-end instance segmentation by only predicting thing classes.

### 3. Methods

#### 3.1. Overall architecture

As illustrated in Figure 2, Panoptic SegFormer consists of three key modules: transformer encoder, location decoder, and mask decoder, where (1) the transformer encoder is applied to refine the multi-scale feature maps given by the backbone, (2) the location decoder is designed to capturing object’s location clues, and (3) the mask decoder is for final classification and segmentation.

During the forward phase, we first feed the input image  $X \in \mathbb{R}^{H \times W \times 3}$  to the backbone network, and obtain the feature maps  $C_3$ ,  $C_4$ , and  $C_5$  from the last three stages, whose resolutions are  $1/8$ ,  $1/16$  and  $1/32$  compared to the input image, respectively. We then project the three feature maps to the ones with 256 channels by a fully-connected (FC) layer, and flatten them into feature tokens  $C'_3$ ,  $C'_4$ , and  $C'_5$ . Here, we define  $L_i$  as  $\frac{H}{2^{i+2}} \times \frac{W}{2^{i+2}}$ , and the shapes of  $C'_3$ ,  $C'_4$ , and  $C'_5$  are  $L_1 \times 256$ ,  $L_2 \times 256$ , and  $L_3 \times 256$ , respectively. Next, using the concatenated feature tokens as input, the transformer encoder outputs the refined features of size  $(L_1 + L_2 + L_3) \times 256$ . After that, we use  $N$  randomly initial-

ized queries to uniformly describe things and stuff. We then embed the location clues (*i.e.* center location and scale (size of mask)). Finally, we adopt a mask-wise strategy to merge the predicted masks into the panoptic segmentation result, which will be introduced in detail in Section 3.6.

#### 3.2. Transformer Encoder

High-resolution and the multi-scale features maps are important for the segmentation task [2, 12, 13]. Since the high computational cost of multi-head attention layer, previous transformer-based methods [15, 17] can only process low-resolution feature map (*e.g.*,  $C_5$  of ResNet) in their encoders, which limits the segmentation performance.

Different from these methods, we employ the deformable attention layer [18] to implement our transformer encoder. Due to the low computational complexity of the deformable attention layer, our encoder can refine and involve positional encoding [25] to high-resolution and multi-scale feature maps  $F$ .

#### 3.3. Location Decoder

Location information plays an important role in distinguishing things with different instance ids in the panoptic segmentation task [11, 12, 34]. Inspired by this, we design a location decoder to introduce the location information (*i.e.*, center location and scale) of things and stuff into the learnable queries.

Specifically, given  $N$  randomly initialized queries and the refined feature tokens generated by transformer encoder, the decoder will output  $N$  location-aware queries. In the training phase, we apply an auxiliary MLP head on top of location-aware queries to predict the center locations and

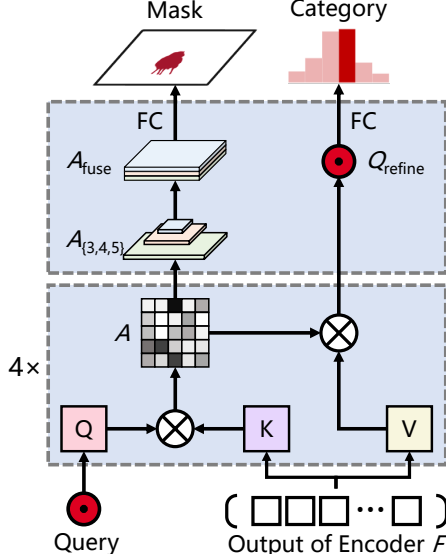


Figure 3: **Architecture of mask decoder.** The attention maps  $A$  are the product of query  $Q$  and key  $K^T$ . We split and reshape multi-scale attention maps to  $A_{\{3,4,5\}}$ , then we upsample and cat these features to  $A_{\text{fuse}}$ . The mask is generated through attention maps with one  $1 \times 1$  conv layer. The category label is predicted from the refined query  $Q_{\text{refine}}$  with one linear projection layer.

scales of the target object, and supervise the prediction with a location loss  $\mathcal{L}_{\text{loc}}$ . Note that, the MLP head is an auxiliary branch, which can be discarded during the inference phase. Since the location decoder does not need to predict the segmentation mask, we implement it with computational and memory efficient deformable attention [18].

### 3.4. Mask Decoder

As shown in Figure 3, the mask decoder is proposed to predict the object category and mask according to the given queries. The queries  $Q$  of the mask decoder is the location-aware queries from the location decoder, and the keys  $K$  and values  $V$  of the mask decoder is the refined feature tokens  $F$  from the transformer encoder. We first pass the queries through 4 decoder layers, and then fetch the attention map  $A \in \mathbb{R}^{N \times h \times (L_1 + L_2 + L_3)}$  and the refined query  $Q_{\text{refine}} \in \mathbb{R}^{N \times 256}$  from the last decoder layer, where  $N$  is the query number,  $h$  is the head number of the multi-head attention layer, and  $L_1 + L_2 + L_3$  is the length of feature tokens  $F$ .

Similar to previous method [15, 16], we directly perform classification through a FC layer on top of the refined query  $Q_{\text{refine}}$  from the last decoder layer.

At the same time, to predict the object mask, we first split and reshape the attention maps  $A$  into attention maps

$A_3$ ,  $A_4$ , and  $A_5$ , which have the same spatial resolution as  $C_3$ ,  $C_4$ , and  $C_5$ . This process can be formulated as:

$$(A_3, A_4, A_5) = \text{Split}(A), \quad A_i \in \mathbb{R}^{\frac{H}{2^{i+2}} \times \frac{W}{2^{i+2}} \times h}, \quad (1)$$

where  $\text{Split}(\cdot)$  denotes the split and reshaping operation. After that, we upsample these attention maps to the resolution of  $H/8 \times W/8$  and concatenate them along the channel dimension, as illustrated in Eqn. 2.

$$A_{\text{fuse}} = \text{Concat}(A_1, \text{Up}_{\times 2}(A_2), \text{Up}_{\times 4}(A_3)). \quad (2)$$

Here,  $\text{Up}_{\times 2}(\cdot)$  and  $\text{Up}_{\times 4}(\cdot)$  mean the 2 times and 4 times bilinear interpolation operations, respectively.  $\text{Concat}(\cdot)$  is the concatenation operation. Finally, based on the fused attention maps  $A_{\text{fuse}}$ , we predict the binary mask through a  $1 \times 1$  convolution.

Note that, because a complete attention map is required to predict segmentation masks, we implement the mask decoder by the common multi-head attention [25], instead of sparse attention layer such as deformable attention [18] and Longformer [35].

### 3.5. Loss Function

During training, follow common practices [15, 36] to search the best bipartite matching between the prediction set  $\hat{Y} = \{\hat{y}_i\}_{i=1}^N$  and the ground truth set  $Y = \{y_i\}_{i=1}^M$ , where  $N \geq M$  is always guaranteed, and the ground truth set  $Y$  is padded with  $\emptyset$  so that the element number is the same as the prediction set  $\hat{Y}$ . Specifically, we utilize Hungarian algorithm [37] to search for the permutation  $\sigma$  with the minimum matching cost which is the sum of the classification loss  $\mathcal{L}_{\text{cls}}$  and the segmentation loss  $\mathcal{L}_{\text{seg}}$ .

The overall loss function of Panoptic SegFormer can be written as:

$$\mathcal{L} = \lambda_{\text{cls}} \mathcal{L}_{\text{cls}} + \lambda_{\text{seg}} \mathcal{L}_{\text{seg}} + \lambda_{\text{loc}} \mathcal{L}_{\text{loc}}, \quad (3)$$

where  $\lambda_{\text{cls}}$ ,  $\lambda_{\text{seg}}$ , and  $\lambda_{\text{loc}}$  are the weights to balance three losses.  $\mathcal{L}_{\text{cls}}$  is the classification loss that is implemented by Focal loss [28], and  $\mathcal{L}_{\text{seg}}$  is the segmentation loss implemented by Dice loss [38].  $\mathcal{L}_{\text{loc}}$  is the location loss as formulated in Eqn. 4:

$$\mathcal{L}_{\text{loc}} = \sum_i^N \mathbb{1}_{\{y_i \neq \emptyset\}} (\mathcal{L}_1(f_c(m_i), \hat{u}_{\sigma(i)}) + \mathcal{L}_1(f_s(m_i), \hat{v}_{\sigma(i)})), \quad (4)$$

where  $\mathcal{L}_1$  is the L1 loss.  $\hat{u}_{\sigma(i)}$  and  $\hat{v}_{\sigma(i)}$  are the predicted center points and scales from the location decoder.  $\sigma(i)$  denotes the  $i^{\text{th}}$  index in the permutation  $\sigma$ .  $f_c(m_i)$  and  $f_s(m_i)$  indicate the center location and scale (size of mask that normalized by the size of the image) of the target mask  $m_i$ , respectively.  $\mathbb{1}_{\{y_i \neq \emptyset\}}$  indicates that only pairs included real ground truth are taken into account.



---

**Algorithm 1: Mask-Wise Merging**

---

```
def MaskWiseMergeing(c, s, m):  
    # category  $c \in \mathbb{R}^N$   
    # confidence score  $s \in \mathbb{R}^N$   
    # mask  $m \in \mathbb{R}^{N \times H \times W}$   
    SemMsk = np.zeros(H, W)  
    IdMsk = np.zeros(H, W)  
    order = np.argsort(-s)  
    id = 0  
    for i in order:  
        # drop low quality results  
        if s[i] < thrcls:  
            continue  
        # drop overlaps  
        mi = m[i] & (SemMsk > 0)  
        SemMsk[mi] = c[i]  
        if isThing(c[i]):  
            IdMsk[mi] = id  
            id += 1  
    return SemMsk, IdMsk
```

---

### 3.6. Mask-Wise Inference

Panoptic Segmentation requires each pixel to be assigned a category label (or void) and instance id (id is ignored for stuff) [1]. One commonly used post-processing method is the heuristic procedure [1], which adopts a NMS-like procedure [1] to generate the non-overlapping instance segments for things and we call it as mask-wise strategy here. The heuristic procedure also uses pixel-wise argmax strategy for stuff and resolves overlap between things and stuff in favor of the thing classes. Recent methods [15–17] directly use pixel-wise strategy directly to uniformly merge the results of things and stuff. Although pixel-wise argmax strategy is conceptually simple, we observe that it consistently produces results with noise due to the abnormally extreme pixel values. To this end, we adopt the mask-wise strategy to generate non-overlap results for stuff based on the heuristic procedure, instead of taking the pixel-wise strategy. However, we equally treat things and stuff and solve the overlaps among all masks by their confidence scores instead of favoring things over stuff in the heuristic procedure, which marks a difference between our approach and [1].

As illustrated in Algorithm 1, mask-wise merging strategy takes  $c$ ,  $s$ , and  $m$  as input, which denote the predicted categories, confidence scores, and segmentation masks, respectively, and output a semantic mask  $\text{SemMsk}$  and a instance id mask  $\text{IdMsk}$ , to assign a category label and a instance id to each pixel. Specifically,  $\text{SemMsk}$  and  $\text{IdMsk}$  are first initialized by zeros. Then, we sorted prediction results in descending order of confidence score, and fill the sorted predicted masks to  $\text{SemMsk}$  and  $\text{IdMsk}$ . Note that, the results with confidence scores below  $\text{thr}_{\text{cls}}$  will be discarded, and the overlaps with lower confidence score will

be removed to generate non-overlap panoptic results. In the end, category label and instance id (only things) is added.

## 4. Experiments

We evaluate Panoptic SegFormer on COCO [21], comparing it with several state-of-the-art methods. We provide the main results of panoptic segmentation and some visualization results. We also report the results of instance segmentation.

### 4.1. Datasets

We perform experiments on COCO 2017 datasets [21] without external data. The COCO dataset contains 118K training images and 5k validation images, and it contains 80 things and 53 stuff.

### 4.2. Implementation Details

Our settings mainly follow DETR and Deformable DETR for simplicity. Specially, we use Channel Mapper [42] to map dimensions of the backbone’s outputs to 256. The location decoder contains 6 deformable attention layers, and the mask decoder contains 4 vanilla cross-attention layers. The hyper-parameters in deformable attention are the same as Deformable DETR [18]. We train our models with 50 epochs, a batch size of 1 per GPU, a learning rate of  $1.8 \times 10^{-4}$  (decayed at the 40th epoch by a factor of 0.1, learning rate multiplier of the backbone is 0.1). We use a multi-scale training strategy with the maximum image-side not exceeding 1333 and the minimum image size varying from 480 to 800. The number of queries  $N$  is set to 400.  $\lambda_{\text{cls}}$ ,  $\lambda_{\text{seg}}$ , and  $\lambda_{\text{loc}}$  in Equation 3 are set to 1, 1, 5, respectively. we employ threshold 0.5 to obtain binary masks from soft masks. Threshold  $\text{thr}_{\text{cls}}$  used to filter low-quality results is 0.3. The PVTv2 [40] is pre-trained on ImageNet-1K [43] set. All experiments are trained on one NVIDIA DGX node with 8 Tesla V100 GPUs. For our largest model Panoptic SegFormer (PVTv2-B5), we use 4 DGX nodes to shorten training time.

**Panoptic segmentation.** We conduct experiments on COCO val set and test-dev set. In Tables 1 and 2, we report our main results, comparing with other state-of-the-art methods. Panoptic SegFormer attains 50.0% PQ on COCO val with ResNet-50 as the backbone and single-scale input, and it surpasses previous methods Panoptic-FCN [13] and DETR [15] over 6.4% PQ and 6.6% PQ, respectively. Except for the remarkable effect, the training of Panoptic SegFormer is efficient. Under  $1\times$  training strategy (12 epochs) and ResNet-50 as the backbone, Panoptic SegFormer achieves 46.4% PQ that can be on par with 46.5% PQ of MaskFormer[17] that training 300 epochs. Enhanced by powerful vision transformer backbone PVTv2-B5 [40], Panoptic SegFormer attains a new record of 54.4%

Method	Backbone	Epochs	PQ	PQ <sup>th</sup>	PQ <sup>st</sup>	#Param	FLOPs
Panoptic FPN [2]	R50-FPN [24, 39]	36	41.5	48.5	31.1	-	-
SOLOv2 [12]	R50-FPN	36	42.1	49.6	30.7	-	-
DETR [15]	R50	~ 150 + 25	43.4	48.2	36.3	42.8M	137G
Panoptic FCN [13]	R50-FPN	36	43.6	49.3	35.0	37.0M	244G
K-Net [14]	R50-FPN	36	45.1	50.3	37.3	-	-
MaskFormer [17]	R50	300	46.5	51.0	39.8	45.0M	181G
DETR [15]	R101	~ 150 + 25	45.1	50.5	37.0	61.8M	157G
Max-Deeplab-S [16]	Max-S	54	48.4	53.0	41.5	61.9M	162G
MaskFormer [17]	R101	300	47.6	52.5	40.3	64.0M	248G
Max-Deeplab-L [16]	Max-L	54	51.1	57.0	42.2	451.0M	1846G
MaskFormer [17]	Swin-L <sup>†</sup> [20]	300	52.7	58.5	44.0	212.0M	792G
Panoptic SegFormer	R50	12	46.4	52.6	37.0	47.0M	246G
Panoptic SegFormer	R50	50	50.0	56.1	40.8	47.0M	246G
Panoptic SegFormer	R101	50	50.4	56.3	41.6	65.9M	322G
Panoptic SegFormer	PVTv2-B0 [40]	50	49.6	55.5	40.6	22.2M	156G
Panoptic SegFormer	PVTv2-B2 [40]	50	52.6	58.7	43.3	41.6M	219G
Panoptic SegFormer	PVTv2-B5 [40]	50	54.1	60.4	44.6	100.9M	391G

Table 1: **Experiments on COCO val set.** Panoptic SegFormer achieves 50.0% PQ on COCO val with ResNet-50 as backbone, surpasses previous methods such as DETR [15] and Panoptic FCN [17] over 6.6% PQ and 6.4% PQ respectively. Under training for 12 epochs, Panoptic SegFormer can achieve 46.4% PQ, which is comparable with 46.5% PQ of MaskFormer [17] that training for 300 epochs. <sup>†</sup> notes that backbones are pre-trained on ImageNet-22K.

Method	Backbone	Epochs	PQ	PQ <sup>th</sup>	PQ <sup>st</sup>	#Param	FLOPs
Panoptic FPN [2]	R101-FPN	36	43.5	50.8	32.5	-	-
DETR [15]	R101	~ 150 + 25	46.0	-	-	61.8M	157G
Panoptic FCN [13]	R101-FPN	36	45.5	51.4	36.4	56.0M	310G
K-Net [14]	R101-FPN	36	47.0	52.8	38.2	-	-
Max-Deeplab-S [16]	Max-S [16]	54	49.0	54.0	41.6	61.9M	162G
K-net [14]	Swin-L <sup>†</sup>	36	52.1	58.2	42.8	-	-
Max-Deeplab-L [16]	Max-L [16]	54	51.3	57.2	42.4	451.0M	1846G
Innovation [22]	ensemble	-	53.5	61.8	41.1	-	-
Panoptic SegFormer	R50	50	50.0	56.2	40.8	47.0M	246G
Panoptic SegFormer	R101	50	50.9	57.1	41.4	65.9M	322G
Panoptic SegFormer	PVTv2-B5 [40]	50	54.4	61.1	44.3	100.9M	391G

Table 2: **Experiments on COCO test-dev set.** With PVTv2-B5 [40] as backbone, Panoptic SegFormer achieves 54.4% PQ on COCO test-dev, surpassed previous SOTA methods Max-Deeplab-L [16] and competition-level methods Innovation [22] over 3.1% PQ and 0.9% PQ respectively with fewer parameters and computation cost.

PQ on COCO test-dev without TTA, surpassing Max-Deeplab[16] over 3.1% PQ. Our method even surpasses the previous competition-level method Innovation [22] over 0.8 % PQ <sup>2</sup>. Figure 4 shows some visualization results on the COCO val set. These original images are highly crowded or occluded scenarios, and our Panoptic SegFormer still can predict convincing results.

**Instance segmentation.** In Table 3, we report our instance segmentation results on COCO test-dev set. For a fair comparison, we use 300 queries for instance segmentation and only things data is used. With ResNet-50 as the backbone and single scale input, Panoptic SegFormer achieves 41.7 mask AP, surpassing previous state-of-the-methods HTC [41] and QueryInst [32] over 1.6 AP and 1.1 AP, respectively.

<sup>2</sup>We only compare methods and results that do not use external data.

Method	Backbone	Epochs	AP <sup>seg</sup>	AP <sup>seg</sup> <sub>S</sub>	AP <sup>seg</sup> <sub>M</sub>	AP <sup>seg</sup> <sub>L</sub>
Mask R-CNN [29]	R50-FPN	36	37.5	21.1	39.6	48.3
SOLOv2 [12]	R50-FPN	36	38.8	16.5	41.7	56.2
SOLQ (300 queries) [31]	R50	50	39.7	21.5	42.5	53.1
HTC [41]	R50-FPN	36	40.1	23.3	42.1	52.0
QueryInst(300 queries) [32]	R50-FPN	36	40.6	<b>23.4</b>	42.5	52.8
Panoptic SegFormer (300 queries)	R50	50	<b>41.7</b>	21.9	<b>45.3</b>	<b>56.3</b>

Table 3: **Instance segmentation experiments on COCO test-dev set.** When training with things only, Panoptic SegFormer can perform instance segmentation. With ResNet-50 as backbone, Panoptic SegFormer achieves 41.7 mask AP on COCO test-dev, which is 1.6 AP higher than HTC [41].

Method	Backbone	#Param	FLOPs	Fps	Memory
Deformable DETR*[18,42]	R50	39.8M	195G	15	4567M
Panoptic SegFormer	R50	47.0M	246G	13	7722M
Panoptic SegFormer	R101	65.9M	322G	10	8396M
Panoptic SegFormer	PVTv2-B5	100.9M	391G	5	23112M

Table 4: Deformable-DETR\* is implemented in MMDet [42] and we use the same encoder with them. Data is measured from the same platform. FLOPs are computed on input images with a size of 1200×800, Frame-per-second (Fps) is measured on a Tesla V100 GPU with a batch size of 1 by taking the average runtime on the entire val set. We obtain the memory consuming data during the training phase with a batch size of 1.

**visualization of attention maps** Different from previous methods, our results are generated through multi-scale multi-head attention maps. Figure 5 shows some samples of multi-head attention maps. Through a multi-head attention mechanism, different heads of one query learn their own attention preference. We observe that some heads pay attention to foreground regions, some heads prefer boundaries, and others prefer background regions. This shows that each mask is generated by considering various comprehensive information in the image.

### 4.3. Complexity of Panoptic SegFormer

We show model complexity and inference efficiency in Table 4, and we can see that Panoptic SegFormer can achieve state-of-the-art performance on panoptic segmentation with acceptable inference speed.

## 5. Conclusion

We propose a concise model named Panoptic SegFormer by unifying the processing workflow of things and stuff. Panoptic SegFormer can surpass previous methods with a large margin and demonstrate the superiority of treating things and stuff with the same recipe.

## References

- [1] Alexander Kirillov, Kaiming He, Ross Girshick, Carsten Rother, and Piotr Dollár. Panoptic segmentation. In *CVPR*, 2019. 1, 2, 5
- [2] Alexander Kirillov, Ross Girshick, Kaiming He, and Piotr Dollár. Panoptic feature pyramid networks. In *CVPR*, 2019. 1, 2, 3, 6
- [3] Jiawei Ren, Cunjun Yu, Zhongang Cai, Mingyuan Zhang, Chongsong Chen, Haiyu Zhao, Shuai Yi, and Hongsheng Li. Refine: Prediction fusion network for panoptic segmentation. In *AAAI*, 2021. 1
- [4] Yuwen Xiong, Renjie Liao, Hengshuang Zhao, Rui Hu, Min Bai, Ersin Yumer, and Raquel Urtasun. Upsnet: A unified panoptic segmentation network. In *CVPR*, 2019. 1, 2
- [5] Siyuan Qiao, Liang-Chieh Chen, and Alan Yuille. Detectors: Detecting objects with recursive feature pyramid and switchable atrous convolution. In *CVPR*, 2021. 1
- [6] Tien-Ju Yang, Maxwell D Collins, Yukun Zhu, Jyh-Jing Hwang, Ting Liu, Xiao Zhang, Vivienne Sze, George Papandreou, and Liang-Chieh Chen. Deeperlab: Single-shot image parser. *arXiv:1902.05093*, 2019. 1
- [7] Naiyu Gao, Yanhu Shan, Yupei Wang, Xin Zhao, Yanan Yu, Ming Yang, and Kaiqi Huang. SSAP: Single-shot instance segmentation with affinity pyramid. In *ICCV*, 2019. 1
- [8] Ujwal Bonde, Pablo F Alcantarilla, and Stefan Leutenegger. Towards bounding-box free panoptic segmentation. In *DAGM German Conference on Pattern Recognition*, 2020. 1
- [9] Bowen Cheng, Maxwell D Collins, Yukun Zhu, Ting Liu, Thomas S Huang, Hartwig Adam, and Liang-Chieh Chen. Panoptic-deeplab: A simple, strong, and fast baseline for bottom-up panoptic segmentation. In *CVPR*, 2020. 1

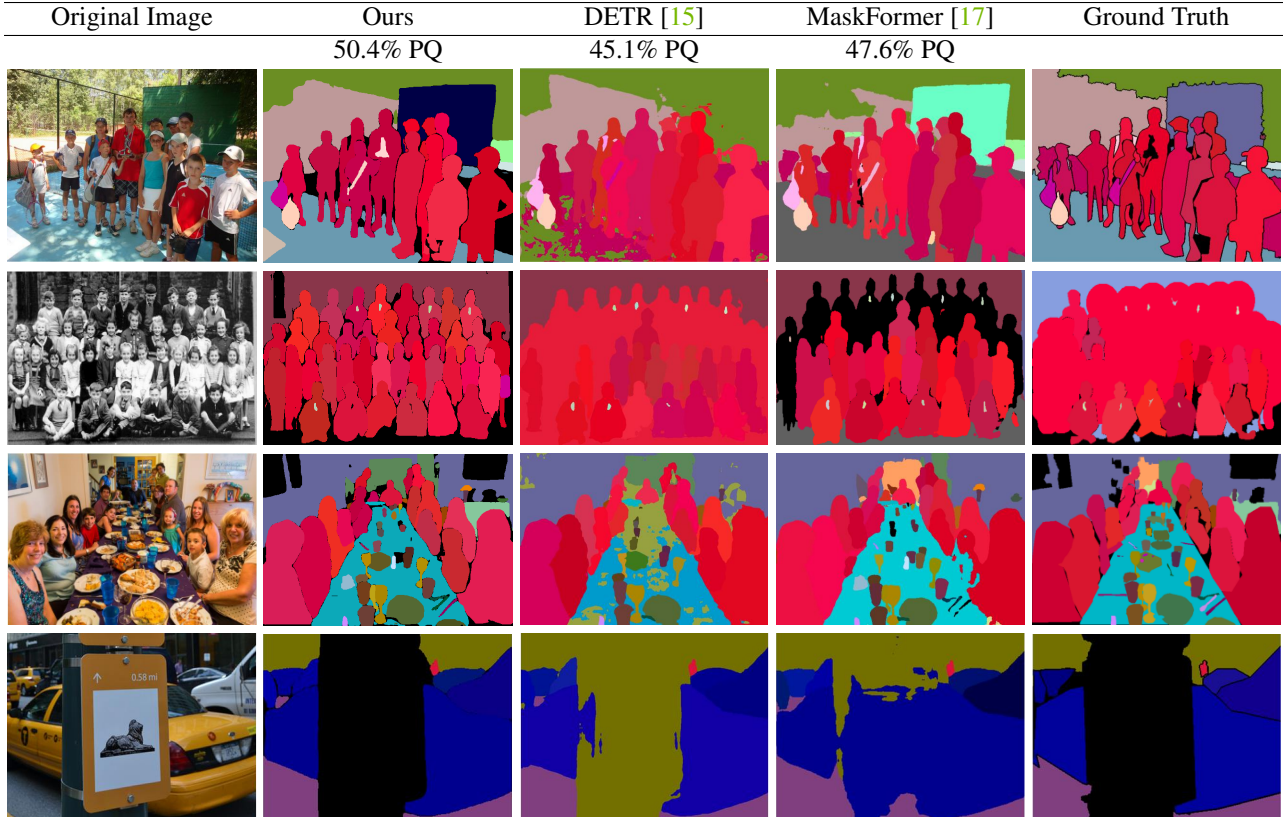


Figure 4: **Comparing visualization results of Panoptic SegFormer with other methods on the COCO val set.** For a fair comparison, all results are generated with ResNet-101 [24] as the backbone. The second and fourth row results show that our method still performs well in highly crowded or occluded scenes. Benefits from our mask-wise inference strategy, our results have few artifacts, which often appear in the results of DETR [15] (e.g., dining table of the third row).

- [10] Huiyu Wang, Yukun Zhu, Bradley Green, Hartwig Adam, Alan Yuille, and Liang-Chieh Chen. Axial-deeplab: Stand-alone axial-attention for panoptic segmentation. In *ECCV*, 2020. 1
- [11] Zhi Tian, Chunhua Shen, and Hao Chen. Conditional convolutions for instance segmentation. In *ECCV*, 2020. 1, 2, 3
- [12] Xinlong Wang, Rufeng Zhang, Tao Kong, Lei Li, and Chunhua Shen. SOLOv2: Dynamic and fast instance segmentation. *NeurIPS*, 2020. 1, 2, 3, 6, 7
- [13] Yanwei Li, Hengshuang Zhao, Xiaojuan Qi, Liwei Wang, Zeming Li, Jian Sun, and Jiaya Jia. Fully convolutional networks for panoptic segmentation. In *CVPR*, 2021. 1, 2, 3, 5, 6
- [14] Wenwei Zhang, Jiangmiao Pang, Kai Chen, and Chen Change Loy. K-net: Towards unified image segmentation. *arXiv:2106.14855*, 2021. 1, 6
- [15] Nicolas Carion, Francisco Massa, Gabriel Synnaeve, Nicolas Usunier, Alexander Kirillov, and Sergey Zagoruyko. End-to-end object detection with transformers. In *ECCV*, 2020. 1, 2, 3, 4, 5, 6, 8
- [16] Huiyu Wang, Yukun Zhu, Hartwig Adam, Alan Yuille, and Liang-Chieh Chen. Max-deeplab: End-to-end panoptic segmentation with mask transformers. In *CVPR*, 2021. 1, 2, 4, 5, 6
- [17] Bowen Cheng, Alexander G Schwing, and Alexander Kirillov. Per-pixel classification is not all you need for semantic segmentation. *arXiv:2107.06278*, 2021. 1, 2, 3, 5, 6, 8
- [18] Xizhou Zhu, Weijie Su, Lewei Lu, Bin Li, Xiaogang Wang, and Jifeng Dai. Deformable detr: Deformable transformers for end-to-end object detection. In *ICLR*, 2020. 1, 2, 3, 4, 5, 7
- [19] Wenhai Wang, Enze Xie, Xiang Li, Deng-Ping Fan, Kaitao Song, Ding Liang, Tong Lu, Ping Luo, and Ling Shao. Pyramid Vision Transformer: A versatile backbone for dense prediction without convolutions. In *ICCV*, 2021. 1
- [20] Ze Liu, Yutong Lin, Yue Cao, Han Hu, Yixuan Wei, Zheng Zhang, Stephen Lin, and Baining Guo. Swin transformer: Hierarchical vision transformer using shifted windows. *ICCV*, 2021. 1, 6
- [21] Tsung-Yi Lin, Michael Maire, Serge Belongie, James Hays, Pietro Perona, Deva Ramanan, Piotr Dollár, and C Lawrence



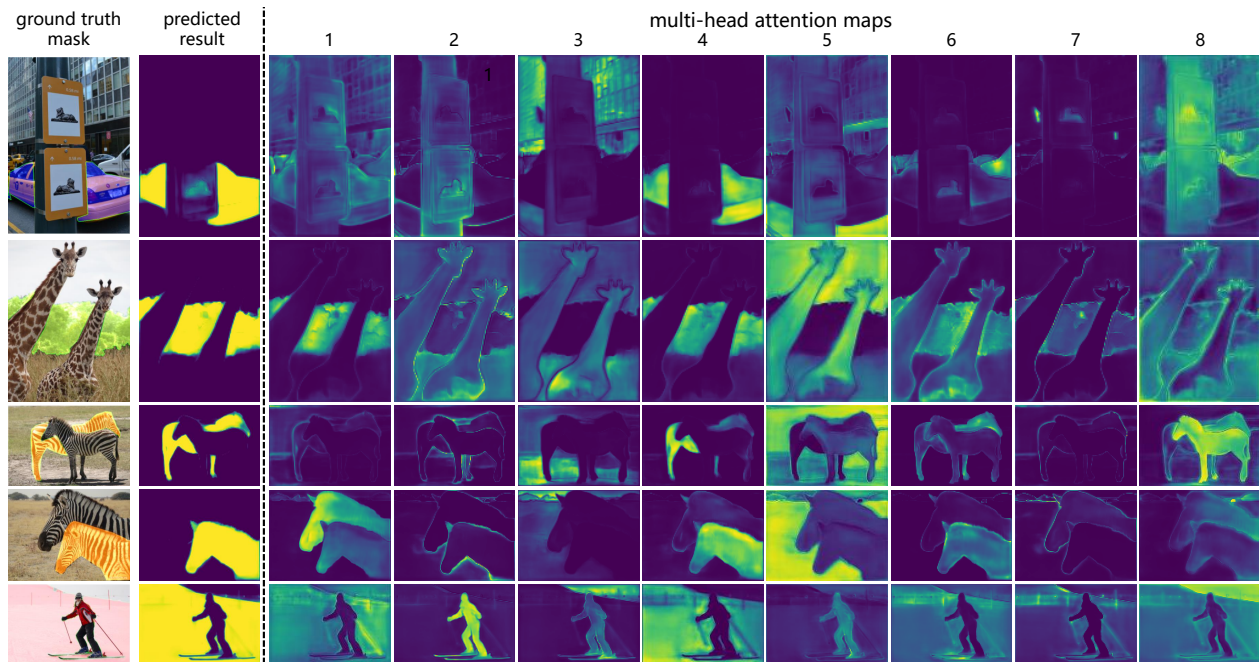


Figure 5: **Visualization of multi-head attention maps and corresponding outputs from mask decoder.** Different heads have different preferences. Head 4 and Head 1 pay attention to foreground regions, and Head 8 prefers regions that occlude foreground. Head 5 always pays attention to the background that is around the foreground. Through the collaboration of these heads, Panoptic SegFormer can predict accurate masks. The 3rd row shows an impressive result of a horse that is highly obscured by the other horse.

- Zitnick. Microsoft coco: Common objects in context. In *ECCV*, 2014. 2, 5
- [22] Chongsong Chen, Jiawei Ren, Daisheng Jin, Zhongang Cai, Cunjun Yu, Bairun Wang, Mingyuan Zhang, and Jinyi Wu. Joint coco and mapillary workshop at iccv 2019: Coco panoptic segmentation challenge track technical report: Panoptic htc with class-guided fusion. *SHR*, 56(84.1):67–2. 2, 6
- [23] Yanwei Li, Xinze Chen, Zheng Zhu, Lingxi Xie, Guan Huang, Dalong Du, and Xingang Wang. Attention-guided unified network for panoptic segmentation. In *CVPR*, 2019. 2
- [24] Kaiming He, Xiangyu Zhang, Shaoqing Ren, and Jian Sun. Deep residual learning for image recognition. In *CVPR*, 2016. 2, 6, 8
- [25] Ashish Vaswani, Noam Shazeer, Niki Parmar, Jakob Uszkoreit, Llion Jones, Aidan N Gomez, Łukasz Kaiser, and Illia Polosukhin. Attention is all you need. In *NIPS*, 2017. 2, 3, 4
- [26] Shen Wang, Tao Liu, Huanyu Liu, Yuchen Ma, Zeming Li, Zhicheng Wang, Xinyu Zhou, Gang Yu, Erjin Zhou, Xiangyu Zhang, et al. Joint coco and mapillary workshop at iccv 2019: Panoptic segmentation challenge track technical report: Explore context relation for panoptic segmentation. In *ICCV Workshop*, 2019. 2
- [27] Shaoqing Ren, Kaiming He, Ross Girshick, and Jian Sun. Faster r-cnn: Towards real-time object detection with region proposal networks. *NIPS*, 2015. 2
- [28] Tsung-Yi Lin, Priya Goyal, Ross Girshick, Kaiming He, and Piotr Dollár. Focal loss for dense object detection. In *ICCV*, 2017. 2, 4
- [29] Kaiming He, Georgia Gkioxari, Piotr Dollár, and Ross Girshick. Mask R-CNN. In *ICCV*, 2017. 2, 7
- [30] Brandon Yang, Gabriel Bender, Quoc V. Le, and Jiquan Ngiam. Condconv: Conditionally parameterized convolutions for efficient inference. In *NeurIPS*, 2019. 2
- [31] Bin Dong, Fangao Zeng, Tiancai Wang, Xiangyu Zhang, and Yichen Wei. Solq: Segmenting objects by learning queries. *arXiv:2106.02351*, 2021. 2, 7
- [32] Yuxin Fang, Shusheng Yang, Xinggang Wang, Yu Li, Chen Fang, Ying Shan, Bin Feng, and Wenyu Liu. Queryinst: Parallely supervised mask query for instance segmentation. *arXiv:2105.01928*, 2021. 3, 6, 7
- [33] Peize Sun, Rufeng Zhang, Yi Jiang, Tao Kong, Chenfeng Xu, Wei Zhan, Masayoshi Tomizuka, Lei Li, Zehuan Yuan, Changhu Wang, et al. Sparse R-CNN: End-to-end object detection with learnable proposals. In *CVPR*, 2021. 3
- [34] Xinlong Wang, Tao Kong, Chunhua Shen, Yuning Jiang, and Lei Li. Solo: Segmenting objects by locations. In *ECCV*, 2020. 3

- [35] Iz Beltagy, Matthew E. Peters, and Arman Cohan. Longformer: The long-document transformer. *arXiv:2004.05150*, 2020. 4
- [36] Russell Stewart, Mykhaylo Andriluka, and Andrew Y Ng. End-to-end people detection in crowded scenes. In *CVPR*, 2016. 4
- [37] Harold W Kuhn. The hungarian method for the assignment problem. *Naval research logistics quarterly*, 2(1-2):83–97, 1955. 4
- [38] Fausto Milletari, Nassir Navab, and Seyed-Ahmad Ahmadi. V-net: Fully convolutional neural networks for volumetric medical image segmentation. In *International conference on 3D vision (3DV)*, 2016. 4
- [39] Tsung-Yi Lin, Piotr Dollár, Ross Girshick, Kaiming He, Bharath Hariharan, and Serge Belongie. Feature pyramid networks for object detection. In *CVPR*, 2017. 6
- [40] Wenhai Wang, Enze Xie, Xiang Li, Deng-Ping Fan, Kaitao Song, Ding Liang, Tong Lu, Ping Luo, and Ling Shao. Pvtv2: Improved baselines with pyramid vision transformer. *arXiv:2106.13797*, 2021. 5, 6
- [41] Kai Chen, Jiangmiao Pang, Jiaqi Wang, Yu Xiong, Xiaoxiao Li, Shuyang Sun, Wansen Feng, Ziwei Liu, Jianping Shi, Wanli Ouyang, et al. Hybrid task cascade for instance segmentation. In *CVPR*, 2019. 6, 7
- [42] Kai Chen, Jiaqi Wang, Jiangmiao Pang, Yuhang Cao, Yu Xiong, Xiaoxiao Li, Shuyang Sun, Wansen Feng, Ziwei Liu, Jiarui Xu, Zheng Zhang, Dazhi Cheng, Chenchen Zhu, Tianheng Cheng, Qijie Zhao, Buyu Li, Xin Lu, Rui Zhu, Yue Wu, Jifeng Dai, Jingdong Wang, Jianping Shi, Wanli Ouyang, Chen Change Loy, and Dahua Lin. MMDetection: Open MMLab detection toolbox and benchmark. *arXiv:1906.07155*, 2019. 5, 7
- [43] Jia Deng, Wei Dong, Richard Socher, Li-Jia Li, Kai Li, and Li Fei-Fei. Imagenet: A large-scale hierarchical image database. In *CVPR. Ieee*, 2009. 5